Ann. Geophys. Discuss., https://doi.org/10.5194/angeo-2018-89
Manuscript under review for journal Ann. Geophys.
Discussion started: 28 August 2018

Annales Geophysicae Discussions
Open Access
EGU

A new scenario applying traffic flow analogy to poleward expansion of auroras

Osuke Saka

Office Geophysik, Ogoori, Japan

Abstract

An auroral ionosphere is generally incompressive and non-uniform medium with anisotropic conductivities. Compressibility may occur, however, following the onset of field line dipolarization. This behavior can happen when; (1) Westward directing electric fields transmitted from the dipolarization region accumulate both electrons and ions in equatorward latitudes in F region. (2) The mobility difference of electrons and ions in E region produces electrostatic potential in a quasi-neutral condition, positive in higher latitudes and negative in lower latitudes. (3) Density modulation in F region excites ion acoustic wave propagating along the field lines towards the magnetosphere. (4) The ion acoustic wave stops in the ionosphere for about 4 min because of a low phase velocity (~1.6 km/s). During this compressive interval, density accumulation in equatorward latitudes expands upstream to form a poleward expansion of auroras analogous to upstream propagation of a shock in traffic flow on crowded roads. Electrostatic potential produced in the E region generates field-aligned currents and closing Pedersen currents to retain electrostatic potential in a quasi-neutral ionosphere. The ion acoustic wave produces upward electric fields along the field lines in accordance with the Boltzmann relation which contributed to the ion upflow at topside ionosphere.

1. Introduction

"Auroras and solar corona observed at the solar eclipse are optical phenomena unique in space physics.

Ann. Geophys. Discuss., https://doi.org/10.5194/angeo-2018-89
Manuscript under review for journal Ann. Geophys.
Discussion started: 28 August 2018

Annales Geophysicae Discussions

With sufficient knowledge about the underlying physical processes, once auroras have been captured by a highly sensitive imager they provide an unexpected wealth of information about plasma environment of the Earth" (copied from [Oguti, 2010]). As one of several unanswered questions involving poleward expansion, plasma drifts in the ionosphere observed by the balloon-measured electric fields [Kelley et al., 1971], by the Ba releases [Haerendel, 1972] and by radar observations [Nielsen and Greenwald, 1978] were opposite to the expanding direction of auroras. To account for the difference in propagation directions, it was suggested that auroras were directly connected to the reconnecting flux tube moving tailward in plasma sheet. The mismatch in the time history of the aurora has been a continuing object of debate [Lui and Rostoker, 2000].

In this report, we present a new scenario to explain differing directions of plasma drifts in the poleward expansion of aurora by assuming compressibility of the ionosphere. It has been suggested that incompressibility and current continuity are inherent electromagnetic properties of the ionosphere. In the incompressive ionosphere, current continuity generates polarization charge and associated field-aligned currents (FACs) along the boundary of the conductivity discontinuity and locally modify the electric fields to enhance the current intensity along a high conductivity strip, referred to as Cowling Channel [Baumjohann, 1983]. The ionospheric currents close not only horizontally in the ionosphere but also in the magnetosphere via FACs through which the magnetosphere and ionosphere is coupled (MI-coupling). The electromagnetic processes associated with auroras have been discussed in this MI-coupling scenario. We will note that incompressibility can be violated for a short interval following the dipolarization onset, and show that the compressibility led to the poleward expansion of auroras and produced parallel electric fields at the topside ionosphere by the excitation of ion acoustic wave. The compressibility also produced electrostatic potential and field-aligned currents.

2. Transmission of westward electric fields to the ionosphere

It is well known that westward electric fields are produced in the midnight magnetosphere in association with the convection surge [Quinn and Southwood, 1982]. The onset of the convection

Ann. Geophys. Discuss., https://doi.org/10.5194/angeo-2018-89
Manuscript under review for journal Ann. Geophys.
Discussion started: 28 August 2018

Annales Geophysicae Discussions
Open Access
EGU

surge is preceded by the pre-onset interval characterized by the inflow of plasma sheet plasmas towards the equatorial plane [Saka and Hayashi, 2017]. The inflow is accompanied by the high-m waves in all-sky image propagating towards the onset latitudes [Nishimura et al., 2014; Saka et al., 2014]. We assume that strength of the westward electric fields of the surge is of the order of 100 mV/m in the auroral ionosphere, corresponding to 2 mV/m observed in dipolarization front in plasma sheet [Runov et al., 2011]. Westward electric fields in the plasma sheet are transmitted along the field lines to the auroral ionosphere by the guided poloidal mode [Radoski, 1967]. Figure 1 illustrates the earthward transmission of the westward electric fields along the field lines, where the electric fields were confined in latitudes between λ_1 and λ_2, peaked at the center. Drift across the magnetic fields for the *j-th* species ($\mathbf{U}_{j\perp}$) can be written in the F region as [Kelley, 1989],

$$\mathbf{U}_{j\perp} = \frac{1}{B}[\mathbf{E} - \frac{k_B T_j}{q_j}\frac{\nabla n}{n}]\times\hat{\mathbf{B}}. \qquad (1)$$

Here, $\mathbf{E}$ denote electric fields pointing westward and $\hat{\mathbf{B}}$ denotes a unit vector of the magnetic fields B, downward in auroral ionosphere. Symbols k_B, T_j, q_j, and n are the Boltzmann constant, temperature of the *j-th* species, charge of the *j-th* species, and density of electrons (ions), respectively. The electric field of the order of 100 mV/m exceeded the diffusion (second term) by three orders of magnitudes in low temperature ionosphere. The diffusion term can be ignored and $E\times B$ drift predominated in the F region. We calculated numerically the density perturbations using the mass conservation equation,

$$\frac{\partial n}{\partial t} + \frac{\partial}{\partial x}(nU) = 0. \qquad (2)$$

Here n is plasma density, U denotes $E\times B$ drift in the x direction (southward) defined by $e^{-(x/20)^2}$, proportional to the electric field profile. We treated this as one-dimensional case as the surge was assumed to spread wider in longitudes than in latitudes. Density distribution was assumed to be uniform at $T = T_0$ and developed with time as illustrated in the inset. The results show that the plasmas were accumulated in equatorward edge of the electric fields and the density hole was produced in the poleward. Because density accumulation was caused primary by the spatial gradient of the drift

Ann. Geophys. Discuss., https://doi.org/10.5194/angeo-2018-89
Manuscript under review for journal Ann. Geophys.
Discussion started: 28 August 2018

Annales Geophysicae Discussions

79 velocity, we can approximate the equation (2) as,

80 $$\frac{\Delta n}{\Delta t} + n_0 \frac{\Delta U}{\Delta x} = 0 . \qquad (3)$$

81 Substituting $\Delta U = 10^3 ms^{-1}$ and $\Delta x = 10^4 m$, we have $\frac{\Delta n}{\Delta t} = 10^{10} m^3 s^{-1}$ at the background density

82 $n_0 = 10^{11} m^{-3}$. This gives density modulation of the order of $\frac{\Delta n}{n_0} = 100\%$ in ten seconds. The

83 accumulation may continue beyond ten seconds because the lifetime of the dipolarization front seems

84 to be longer [Runov et al., 2011].

85 In the bottom side of the ionosphere (E region), differences in drift velocity of electrons and

86 ions produces electrostatic potential. Drift trajectories in the E region may be written [Kelley, 1989]

87 for electrons by,

88 $$\mathbf{U}_{e\perp} = \frac{1}{B}[\mathbf{E} \times \hat{\mathbf{B}}] \qquad (4)$$

89 and for ions by,

90 $$\mathbf{U}_{i\perp} = b_i[\mathbf{E} + \kappa_i \mathbf{E} \times \hat{\mathbf{B}}] . \qquad (5)$$

91 Here, b_i is mobility of ions defined as $\Omega_i/(B\nu_{in})$, κ_i is defined as Ω_i/ν_{in}. Symbols Ω_i and

92 ν_{in} are ion gyrofrequency and ion-neutral collision frequency, respectively. $\hat{\mathbf{B}}$ denotes a unit vector

93 of the magnetic fields B. To derive equations (4) and (5), pressure gradient term (diffusion) was

94 again ignored. In the E region ($\kappa_i = 0.1$), although the first term of (5) exceeds the second term by

95 one order of magnitudes, electron accumulation in equatorward latitudes by the imposed westward

96 electric fields are produced by the mobility difference of electrons in (4) and the second term of the

97 ions in (5). However, southward electric fields associated with the electron accumulation in lower

98 latitudes increased immediately and simultaneously ion drifts in the first term of (5) increase. If the

99 southward electric fields grew to exceed the westward electric fields by an order of magnitudes, ion

100 drifts in the first term of (5) and electron drifts in (4) balanced to satisfy the quasi-neutrality. This is

101 equivalent to the generation of the Pedersen currents in the ionosphere. The Pedersen currents would

Ann. Geophys. Discuss., https://doi.org/10.5194/angeo-2018-89
Manuscript under review for journal Ann. Geophys.
Discussion started: 28 August 2018

Annales Geophysicae Discussions

have closed to the field-aligned current (FAC) and sustain the steady state electrostatic potential produced by the compression. The electrostatic potential thus produced in auroral ionosphere would contribute to the atmospheric electricity in Antarctica [Kondo, 1970; Minamoto and Kadokura, 2011].

3. Poleward expansion of density accumulation

If the compressed ionospheric plasmas stop in the ionosphere, then question arises regarding the maximum accumulation in the ionosphere. One possible mechanism to suppress the accumulation may be associated with the ionospheric screening that decreased the amplitudes of penetrated westward electric fields. Total electric fields *E*, a sum of the incident and reflected westward electric fields, may be written as $E = 2\Sigma_A/(\Sigma_A + \Sigma_P)$, where Σ_A and Σ_P are Alfven conductance defined by $1/\mu_0 V_A$ and height integrated Pedersen conductance in the ionosphere, respectively [Kan et al., 1982]. Symbols μ_0 and V_A denote magnetic permeability in vacuum and Alfven velocity, respectively. Substituting a typical conductance $\Sigma_A = 10^0 S$, and $\Sigma_P = 10^1 S$, total electric fields decreased at the density peak to 18% of the incident electric fields. Another clue may be found in the polarization electric fields produced by the accumulation itself. The electric fields associated with the accumulation (secondary electric fields), directing southward, grew quickly and increased the amplitudes over the primary westward electric fields. Assuming the convection surge is localized in longitudes, the secondary electric fields generate polarization charge, negative to the east and positive to the west, by the electrons transported towards east. The induced polarization charge decreased westward electric fields and slowed down the flow velocity at the density peak. In addition to the above scenarios, we suggest that excess accumulation of the ionospheric plasmas may be suppressed through the term, $(\mathbf{U}\cdot\nabla)\mathbf{U}$, in the equation of motion. This effect, however, may not be a significant factor in decelerating the equatorward flows, because the electric fields in the ionosphere much exceeded the pressure gradient force. All these possible mechanisms would slow the southward flow at the density peak located to the south of the maximum flow velocity. Latitudinal profile of the resulting southward

Ann. Geophys. Discuss., https://doi.org/10.5194/angeo-2018-89
Manuscript under review for journal Ann. Geophys.
Discussion started: 28 August 2018

Annales Geophysicae Discussions
Open Access
EGU

drifts is illustrated by the dashed line in the upper panel of Figure 2. The slowdown of the drift velocity suppressed the further accumulation while equatorward flow continues. This leads to nonlinear evolution of the density profiles analogous to upstream propagation of a shock in traffic flow [Lighthill and Whitham, 1955].

We will study how these plasmas, which pile up at equatorward latitudes, develop over time. Assuming drift velocity U is a function of the density n, the conservation equation (2) may be written as [Farlow, 1982],

$$\frac{\partial n}{\partial t} + g(n)\frac{\partial n}{\partial x} = 0 . \qquad (6)$$

Here, $g(n) = \frac{dq}{dn}$ and q is a flux defined by $q = nU(n)$. The flux (q)-density (n) curve as illustrated in Figure 3(A) by $q = An(n_0 - n)$ matches drift in the ionosphere where the drift slowed down at the density peak. Here, A is a constant value related to the average drift velocity. Drift velocity is smooth in the range $n < n_c$ whereas the flow decelerates in the range $n > n_c$ and completely stops at $n = n_0$. The conservation equation (6) and flux-density curve in Figure 3(A) show us nonlinear evolutions of the density profile as is illustrated in Figure 3(B). An initial density profile at T=0 shown by solid lines indicates that flow stops completely at x downstream of x_1. At $T=T_1$, the density profile was deformed to a shock indicated by dashed curve in red. A shock front developed at $n = n_c$ where propagation velocity of the kinematic waves, $g(n)$, [Whitham, 1999] changed its sign from positive to negative (Figure 3(A)). The shock front at $x = x_c$ propagated upstream at velocity $U = -A \cdot n_{in}$. If the number densities and fluxes carried to onset latitudes are sufficiently high, then the poleward expansion may be explosive; with quick formation of the shock and a large expansion velocity. The electrostatic potential produced in the E region would have also expanded poleward. This electrostatic potential may produce vortical flows in the F region and loop currents in the E region, which may expand as a shock.

Ann. Geophys. Discuss., https://doi.org/10.5194/angeo-2018-89
Manuscript under review for journal Ann. Geophys.
Discussion started: 28 August 2018

Annales Geophysicae Discussions

152

153 **4. Parallel electric fields associated with density accumulation**

154 The transient compression of the ionospheric plasmas associated with the accumulation by the
155 $E \times B$ drift would excite the ion acoustic wave in the ionosphere travelling along the field lines
156 upward and downward directions from the density peak of the F region. Figure 4(A) shows height
157 distribution of the pre-onset density profile of electrons (black), density profile caused by the
158 accumulation (dashed-red) and its decay associated with the travelling ion acoustic wave (dashed-
159 green). It is assumed that accumulation doubled the electron density profile at the equatorward edge
160 of convection surge from 90 km to 1000 km in altitudes. Electron density profile was plotted using
161 sunspot maximum condition given in Prince and Bostic (1964). The travelling ion acoustic waves,
162 upward and downward, are denoted by vertical arrows. Ion acoustic wave propagating downward may
163 be eventually absorbed in the neutrals, while the upward wave may propagate along the field lines. By
164 assuming that electron motions are determined by the Boltzmann relation in our case, we give the
165 electrostatic potential ϕ of the ion acoustic wave by the relation,

166 $$\delta n_e = -n_e \frac{q\phi}{k_B T_e}, \qquad (7)$$

167 or by [Chen, 1974],

168 $$E_{//} = -\frac{k_B T_e}{q} \frac{\nabla_{//} n_e}{n_e}. \qquad (8)$$

169 Here, k_B is Boltzmann constant, q is electron charge, T_e is electron temperature, n_e is electron
170 density ($n_e = n_i$), and δn_e is perturbed electron density. We will focus only on the upward travelling
171 ion acoustic wave. Equation (8) gives electric field strengths of the order of $0.4\mu V/m$ and
172 $2.0\mu V/m$ for $T_e = 1000K$ and $T_e = 5000K$, respectively, when the e-folding distance of
173 density dropout along the filed lines was 200 km. For ions, however, field-aligned flows in collisional
174 plasmas with gravity force may be given as [Kelley, 1989],

Ann. Geophys. Discuss., https://doi.org/10.5194/angeo-2018-89
Manuscript under review for journal Ann. Geophys.
Discussion started: 28 August 2018

Annales Geophysicae Discussions
Open Access
EGU

$$V_{i//} = b_i E_{//} - D_i \frac{\nabla_{//} n}{n} - \frac{g}{\nu_{in}} . \qquad (9)$$

Here, b_i and D_i denote mobility and diffusion coefficient of ions defined by $\frac{q_i}{M_i \nu_{in}}$ and $\frac{k_B T_i}{M_i \nu_{in}}$, respectively. Symbols, M_i, q_i, ν_{in} and g are ion mass, electric charge of ions, ion-neutral collision frequency and gravity, respectively. To evaluate equation (9), we assumed *1000K* for ion temperatures and the same e-folding distance used in equation (8). Ions are oxygen and ion-neutral collision frequencies for the nighttime sunspot maximum condition given in Prince and Bostic (1964) were used. Parallel electric fields were estimated by the equation (8) for different electron temperatures. Snapshot of the velocity profile in altitudes from 400 km to 800 km are shown in Figure 4(B) for the two cases of electron temperatures, 5000K for black dots and 1000K for red dots. For the low temperature case (1000k), there occurred no ion upflow because the parallel electric fields could not overcome the gravity. We suggest that electron temperatures over 2700K would be needed to excite ion upflow or for excitation of ion acoustic wave propagating upward. Ion velocity increased rapidly above 600 km altitudes and reached 1369 m/s at 800 km when electron temperature increased to 5000K. The velocity of the ion upflow became comparable to the phase velocity of ion acoustic wave (1.6 km/s) at the altitudes of 800 km. This may suggest that an initial perturbation of the ion acoustic wave would have been localized in altitudes below 800 km in the topside ionosphere and stopped there for 4 min because of its slow propagation velocity (1.6 km/s). We conclude that the ion upflow in topside ionosphere was caused primary by the parallel electric fields excited by the upward travelling ion acoustic wave.

7. Summary

Allowing for the compressibility of the ionosphere for a short interval following the dipolarization onset, we proposed a new scenario for the poleward expansion of auroras including

Ann. Geophys. Discuss., https://doi.org/10.5194/angeo-2018-89
Manuscript under review for journal Ann. Geophys.
Discussion started: 28 August 2018

generation of field-aligned currents and parallel electric fields of the ionospheric origin. This scenario partly explains the discrepant time history of the aurora: plasmas drift in the ionosphere opposite to the expanding direction of aurora. We emphasize that the ionosphere is not a mere earthward boundary of the magnetosphere but a source region directly producing magnetospheric processes.

Acknowledgements

The author would like to express his sincere thanks to all the members of Global Aurora Dynamics Campaign (GADC) [Oguti et al., 1988]. We also acknowledge STEP Polar Network (http://step-p.dyndns.org/~khay/).

References

Baumjohann, W.: Ionospheric and field-aligned current systems in the auroral zone: a concise review, Adv.Space Res., 2, 55-62, 1983.

Chen, F.F.: Introduction to plasma physics, Plenum Press, New York, 1974.

Farlow, S.J.: Partial differential equations for scientists and engineers, John Wiley & Sons, Inc., 1982.

Haerendel, G.: Plasma drifts in the auroral ionosphere derived from Barium release, in Earth magnetospheric processes, B.M. McComac (ed), D.Reidel Publishing Company, 246-257, 1972.

Kan, J.R., Longenecker, D.U., and Olson, J.V.: A transient response of Pi2 pulsations, J.Geophys.res., 87, 7483-7488, 1982.

Kelley, M.C., Starr, J.A., and Mozer, F.S.: Relationship between magnetospheric electric fields and the motion of auroral forms, J.Geophys.Res., 76, 5256-5277, 1971.

Kelley, M.C.: The earth's ionosphere: plasma physics and electrodynamics, Academic Press, Inc., 1989.

Kondo, K.: Observations of the atmospheric electric field at Syowa station, Antarctica, Journal of the Meteorological Society of Japan, 48, 452-46, 1970.

226 Lighthill, M.J., and Whitham, G.B.: On kinematic waves. II. A theory of traffic flow on long crowded
227 roads, Proc. R. Soc. Lond. A, 229, 317-345, 1955.
228 Lui, A.T.Y., and Rostoker, G.: Substorm expansion mechanism debated, EOS, 81, 70-73, 2000.
229 Minamoto, Y., and Kadokura, A.: Extracting fair-weather data from atmospheric electric-field
230 observations at Syowa station, Antarctica, Polar Science, 5, 313-318, 2011.
231 Nielsen, E., and Greenwald, R.A.: Variations in ionospheric currents and electric fields in association
232 with absorption spikes during substorm expansion phase, J.Geophys.Res., 83, 5645-5654,
233 1978.
234 Nishimura, Y., Lyons, L.R., Nicolls, M.J., Hampton, D.L., Michell, R.G., Samara, M., Bristow, W.A.,
235 Donovan, E.F., Spanswick, E., Angelopoulos, V., and Mende, S.B.: Coordinated ionospheric
236 observations indicating coupling between preonset flow burst and waves that lead to substorm
237 onset, J.Geophys.Res., 119, doi10.1002/2014JA019773, 2014.
238 Oguti, T., Kitamura, T., and Watanabe, T.: Global aurora dynamics campaign, 1985-1986,
239 J.Geomag.Geoelectr, 40, 485-504, 1988.
240 Oguti, T.: Introduction to auroral physics (in Japanese), Laboratory for Solar-Terrestrial Environment,
241 Nagoya University, 2010.
242 Prince, Jr., C.E., and Bostick, Jr., F.X.: Ionospheric transmission of transversely propagated plane
243 waves at micropulsation frequencies and theoretical power spectrums, 69, 3213-334, 1964.
244 Quinn, J.M., and Southwood, D.J.: Observations of parallel ion energization in he equatorial region,
245 J.Geophys.Res., 87, 10536-10540, 1982.
246 Radoski, H.R.: Highly asymmetric MHD resonances: The guided poloidal mode, J.Geophys.Res., 72,
247 4026-4027, 1967.
248 Runov, A., Angelopoulos, V., Zhou, X.-Z., Zhang, X.-J., Li, S., Plaschke, F., and Bonnell, J.: A
249 THEMIS multicase study of dipolarization fronts in the magnetotail plasma sheet,
250 J.Geophys.Res., 116, A05216, doi:10.1029/2010JA016316, 2011.
251 Saka, O., Hayashi, K., and Thomsen, M.: Pre-onset auroral signatures and subsequent development of
252 substorm auroras: a development of ionospheric loop currents at the onset latitudes, Ann.

Ann. Geophys. Discuss., https://doi.org/10.5194/angeo-2018-89
Manuscript under review for journal Ann. Geophys.
Discussion started: 28 August 2018

Geophys., 32, 1011-1023, 2014.

Saka, O., and Hayashi, K.: Longitudinal expansion of field line dipolarization, J.Atomos.Solar Terr.Phys., 164, 235-242, 2017.

Whitham, G.B.: Linear and nonlinear waves, A Wiley-Interscience Publication, JOHN WILEY & SONS, INC., 1999.

Figure Captions

Fig. 1: Transmission of the westward electric fields along the field lines is illustrated in the flux tube localized between latitudes λ_1 and λ_2. The inset at the lower right corner illustrates the latitudinal profile of the southward drift velocity (U) of the ionospheric plasmas produced by these electric fields and density profiles (n) developed in time from T_0 to T_7 (see text).

Fig.2: Same as inset in Figure 1 but a slowdown of the equatorward drift was considered (see text). The equatorward drift velocity slowed down (dashed curve in upper panel) at the peak of plasma accumulation in lower latitudes (lower panel). The solid curve denotes velocity profile with no slowdown.

Fig. 3: (A) Flux(q)-density(n) curve in ionosphere associated with equatorward drift. Flux was maximum at n_c and diminished at the density peak, n_0. $\frac{\partial q}{\partial n}$ denotes propagation of kinematic waves, positive towards the concentration section and negative away from the concentration. (B) Black curve denoted by T=0 shows the initial density profile. Flow is stopped at x downstream of x_1. Plasmas with density (n_{in}) move into the slowdown section. Dotted red curve shows shock formation at $T=T_1$. Plasmas in the section n_{in} - n_c are accelerating ($\frac{\partial q}{\partial n} > 0$), while plasmas in n_c – n_0 are decelerating ($\frac{\partial q}{\partial n} < 0$) to form the shock front. The shock front propagates upstream at a velocity -A n_{in}.

Ann. Geophys. Discuss., https://doi.org/10.5194/angeo-2018-89
Manuscript under review for journal Ann. Geophys.
Discussion started: 28 August 2018

Annales Geophysicae Discussions Open Access EGU

278

279 Fig 4: (A) Vertical profile of electron number density in pre-onset (black) and vertical profile
280 associated with accumulation (dashed-red) from 90 km to 1000 km in altitudes. The e-folding distance
281 of density decrease is 200 km in altitudes above 400 km. Dashed-green curve denotes a decay of the
282 density accumulation caused by travelling ion acoustic wave along the field lines upward and
283 downward as marked by vertical arrows. (B) Velocity profile in altitudes for ions (oxygen) produced
284 by parallel electric fields $0.4\mu V/m$ (T_e=1000K) in red dots and $2.0\mu V/m$ (T_e=5000K) in black
285 dots. Vertical flows in altitudes from 400 km to 800 km are shown. Flow velocity is positive upward
286 and negative downward.

287

288

289

290

291

292

293

294

295

296

297

298

299

300

301

302

303

304

Ann. Geophys. Discuss., https://doi.org/10.5194/angeo-2018-89
Manuscript under review for journal Ann. Geophys.
Discussion started: 28 August 2018

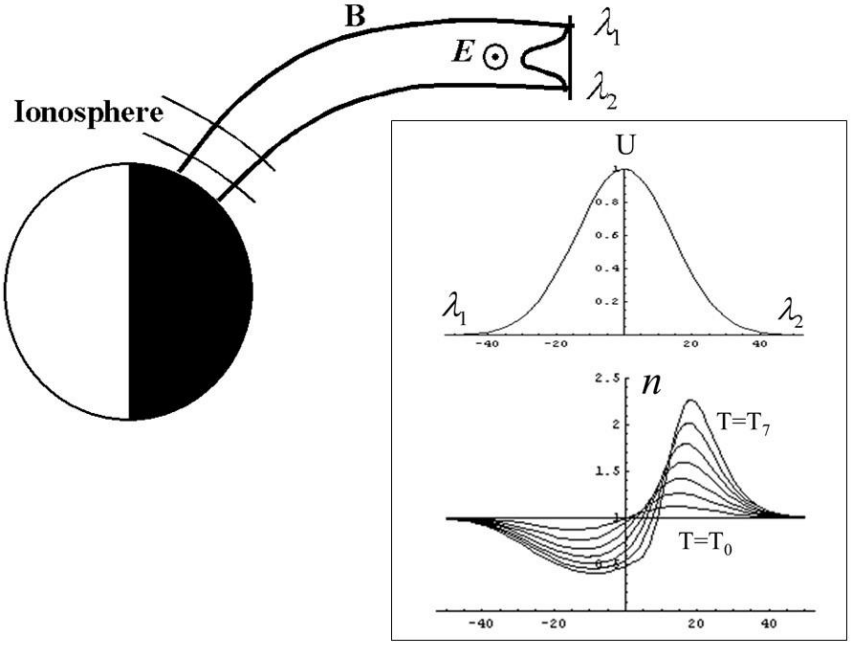

Figure 1

Ann. Geophys. Discuss., https://doi.org/10.5194/angeo-2018-89
Manuscript under review for journal Ann. Geophys.
Discussion started: 28 August 2018

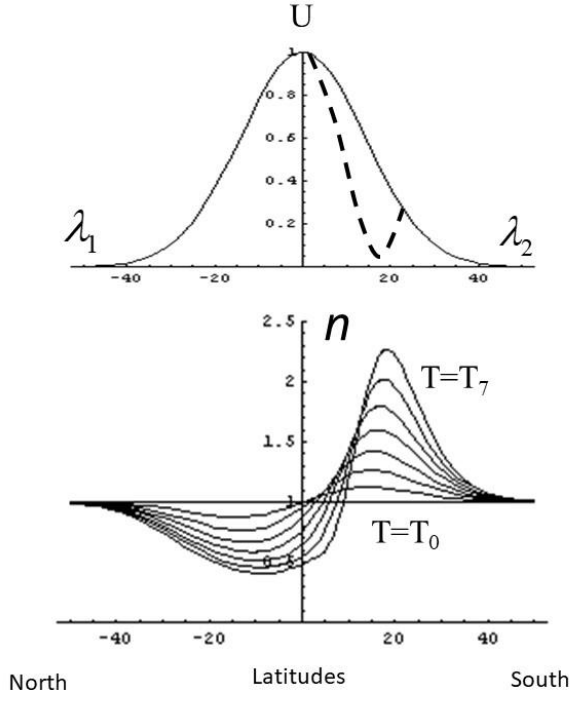

Figure 2

Ann. Geophys. Discuss., https://doi.org/10.5194/angeo-2018-89
Manuscript under review for journal Ann. Geophys.
Discussion started: 28 August 2018

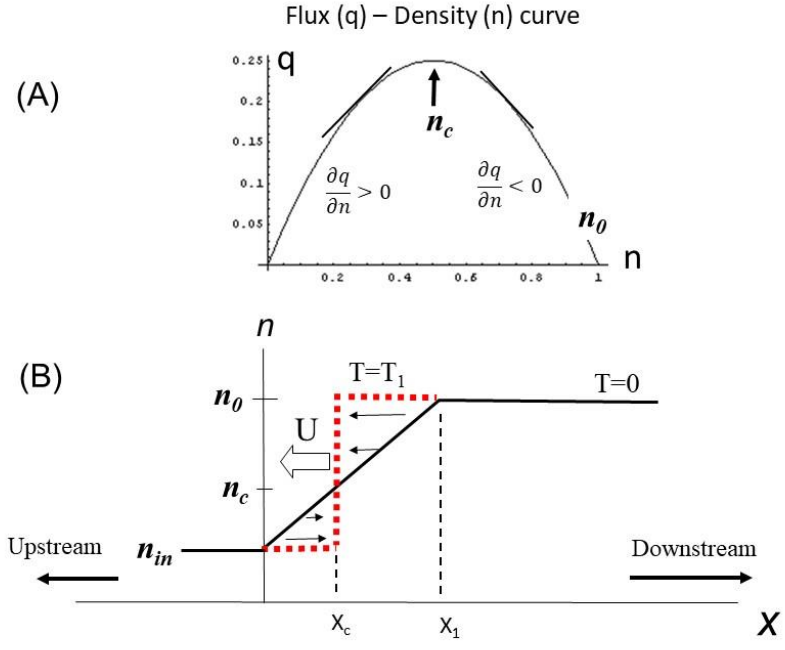

Figure 3

Ann. Geophys. Discuss., https://doi.org/10.5194/angeo-2018-89
Manuscript under review for journal Ann. Geophys.
Discussion started: 28 August 2018

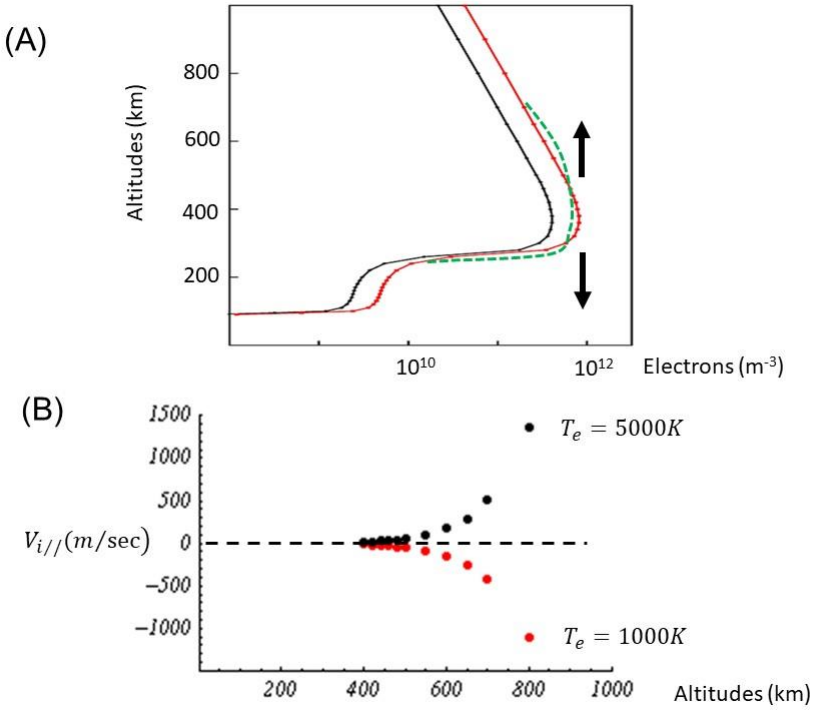

Figure 4